THE JACOBIAN ANALYSIS OF COLOR IMAGE MACHINES

I. CONTINUOUS RELATIONSHIP BETWEEN CONTROL AND COLOR

By

RICHARD D. JUDAY
Tracking and Communications Division
NASA Johnson Space Center
Houston, Texas 77058

and

RICHARD W. NEWTON
Electrical Engineering Department
Texas A&M University
College Station, Texas 77843

January 1986

(NASA-TM-89616) THE JACOBIAN ANALYSIS OF COLOR IMAGE MACHINES. 1: CONTINUOUS RELATIONSHIP BETWEEN CONTROL AND COLOR (NASA) 32 p Avail: NTIS

N87-70442

Unclas
00/35 0079412

THE JACOBIAN ANALYSIS OF COLOR IMAGE MACHINES

I. CONTINUOUS RELATIONSHIP BETWEEN CONTROL AND COLOR

BY

RICHARD D. JUDAY AND RICHARD W. NEWTON

Abstract

In making color imagery from numerical imagery, the details of the quantitative relationship between the vector of control values and the color actually produced are often overlooked. Most of the attention has gone into manipulations of the vector data (stretchings, rotations, etc.) prior to their being converted to color controls, with incomplete consideration for the effects the color image machine will then cause. "Density linearization" is a common method of setting up color machines; in it, a logarithmic relationship is induced between radiance and the control producing it. Density linearization, even if done on only one axis at a time, is a step towards achieving uniformity of color vs. control. However, the off-axis effects are usually neglected, and the visibility of one data component's changes can be masked by other components'. An idealized continuous color image machine is modelled, and the undesirable effects of the off-axis behavior are shown by means of the Jacobian matrix.

One subsequent paper will extend the Jacobian analysis to discrete machines such as dot-matrix printers, and another will offer

the cure for the effects shown here.

A. INTRODUCTION

Simply stated, the objective of a color image machine is to make visible to a human analyst the information contained in numerical data that are used to control the machine. Little is to be found in the image-processing literature on the effects that the machine has in that process, it apparently being assumed that if the data are treated so as to have the appropriate statistics (uncorrelatedness, large variances, etc.), then the data components can be mapped affinely into the control channels of a machine and acceptable color imagery will result. For examples see Madura et al. (1978), Soha et al. (1976), Tajima (1983), and others. The common transforms (HSI, linear stretch, histogram equalization, decorrelation stretching, etc.) all myopically consider data transformations only to the point of their being entered into the controls of the machine. However, as will be shown, even a machine that is noise-free, continuously addressable in its control vector domain, and has exactly the ordinary ideal relationship (e.g. Catmull, 1979) between control and spectral radiance, will nonetheless distort the relationships that exist in the numerical data, if we have a normally-sighted human interpret the data. The color gamut of the machine is ordinarily sufficiently large that the important data vector differences are visually discriminable when thus converted to color, and the imagery will pass a visual examination that is not strict with respect to comparative color differences for various data vector differences. If, however, the comparative color differences are to be analyzed in the visual imagery, then either the data will have to be treated to account for the effects the color machine will have on them, or else the machine will have to be set up to minimize those effects. The purpose of this paper is to show the presence of the effects in even the best-intentioned color machine.

We will consistently use the term "covariance" in the multivariate statistical sense--the expectation of a vector less its mean times the transpose of that difference. We note that covariance is not the same as information, but we posit that the ideal color image machine is one that conveys covariance in its control space uniformly into perceived covariance in the colors seen by the analyst looking at the image. That is, we assume that the operations done on the data prior to their being displayed condition them so that their covariances are what are desired to be seen. For the purposes of this paper, we will ignore adjacency effects, small-field tritanopia, and other aspects of color theory that consider a neighborhood rather than a point in the visual field. With those preliminaries we can use a body of data, theory, and algorithms developed by color metricians to examine the behavior of a color image machine. We refer the reader to Wyszecki and Stiles (1982) for the colorimetry necessary in the rest of the paper.

We note that the term "density linearization" is somewhat loose usage; more accurately one would perhaps use "affine density" or "first-order density".

B. THE MODEL OF A CONTINUOUS ADDITIVE MACHINE

By a model of a color machine we mean the relationship between the color produced at a location in the output image and the vector of controls at the corresponding location in the input image. We will assume that the relationship is not dependent on position in the image, time, or other confounding parameters. The input vector is taken as the usual controls, they being r, g, b (red, green, and blue) all lying in the closed interval zero to unity. We will refer to the space of control vectors as K-space and to the space of numerically expressed colors as C-space.

We take our ideal machine as one that is strictly color-additive--the light that is produced from each of the channels (as by emission from a CRT or reflection from hardcopy film) is literally added in the sense of Grassman's laws. (No CRT or film machine is physically so clean; only a physical system that projects colored images into coincidence onto a screen realizes it.) Suppose that the r control moderates the red primary light, g the green, and b the blue. The spectral radiances of the primaries add, as do the CIE tristimulus values. What remains is to specify the relationship between the control value and the strength of the primary light it causes. We will examine two such; the first has radiance proportional to control, and the second has the logarithm of radiance proportional to control.

1. Linear in radiance

$$T = \sum_{i \in r,g,b} \begin{pmatrix} X_i \\ Y_i \\ Z_i \end{pmatrix} K_i \qquad (1)$$

in which $\underline{T}$ is the tristimulus vector; X, Y, and Z are the CIE tristimulus values; K_i is the i-th component of the control vector; and the i-subscripted tristimulus values are the result of full activation of that primary. For definiteness, we define MTV as the matrix of tristimulus values

$$MTV = \begin{pmatrix} X_R & X_G & X_B \\ Y_R & Y_G & Y_B \\ Z_R & Z_G & Z_B \end{pmatrix} = \begin{pmatrix} 58.79 & 17.92 & 18.31 \\ 28.96 & 60.58 & 10.46 \\ 0.0 & 6.83 & 102.02 \end{pmatrix} \qquad (2)$$

which corresponds to lights of the NTSC-defined chromaticities (Pratt, 1978) for broadcast television, balanced to match the CIE D65 illuminant when all controls are fully activated. These values were used in the calculations for the figures. Then

$$\underline{T} = MTV \bullet \underline{K} \qquad (3)$$

2. Linear in density

This condition is the one most often sought in setting up machines; it is predicated on the Weber-Fechner law, that constant ratios of radiances cause equally-perceptible differences in brightness. Indeed, one-dimensional scales in which the logarithm of radiance is equally spaced present themselves pleasingly to the eye as visually uniform scales. (But we shall see that the fully three-dimensional aspects are less salutary.)

$$I = MTV \bullet \{10^{**}[-D_{max}(1-K_i)]\} \quad (4)$$

Note that if we have density linearization, we cannot turn any primary all the way off, as that would correspond to infinite density (recall that density is the negative base-10 logarithm of the transmittance or reflectance). In the above equation, D_{max} gives the maximum density that is achieved, zero being the minimum, for K_i in its domain. E.g., for $D_{max} = 1$, only a factor of ten is possible for variations in the radiance of any primary.

If the proviso of the Introduction is accepted, that the data to be displayed have been conditioned so that their covariance is what is desired to be made visible, we can extrapolate to say that the ratio of visible discriminability to covariance should be constant throughout the region of data space that is converted into color. That is, we wish for one component of the data vector not to affect the visibility of the variance in another component. To allow an examination of whether this is the case we will need some of the concepts of UCS systems.

A UCS (uniform chromaticity scale) system is a numerical color coordinate system in which the Euclidean metric gives a usable approximation to the visibility of color difference. The familiar "straight-line" distance between the points that represent colors in the UCS space is roughly proportional to the minimum number of barely-perceptible color changes along the set of all color sequences that have the two colors at opposite ends. For a detailed description of line-element theory as applied to color metrics, see Wyszecki and Stiles, 1982). For the purposes of this paper we need only to know that the CIELUV color system is such a transformation of the tristimulus values calculated above that the Euclidean distance between colors so transformed is nearly proportional to how strongly different they appear. The transformation from tristimulus values to the CIELUV coordinates L*, u* and v* is given in the Appendix. The Euclidean metric of color difference is

$$\Delta E = \sqrt{(\Delta L^*)^2 + (\Delta u^*)^2 + (\Delta v^*)^2} .$$

By it and the machine model, we calculate the visible color difference resulting from a control vector change. The unit of color difference is the JND, which stands for "just noticeable difference".

C. THE JACOBIAN MATRIX

Once we have a model for the machine, we can formulate a powerful tool for analyzing the relationship between the data vectors and the colors they evoke. That tool is the Jacobian matrix.

The Jacobian matrix here is exactly as described in any advanced calculus text; viz., it is the matrix of partial derivatives of the UCS color coordinates with respect to the control values. We will assume that the required derivatives exist for our ideal machine, and we will also assume that we are examining small enough control differences (and resulting color differences) that the first-order partial derivatives adequately describe the local behavior. Given an analytic model of our machine it is straightforward to derive the analytic form of the Jacobian matrix, but in fact we took the derivatives by finite differences for the figures shown here. We took small differences in control values and the model-calculated color differences in the CIELUV coordinates; their ratio gives the derivatives. Step sizes were chosen small enough to stay locally within linear behavior, large enough to avoid trouble with digital computation precision.

The Jacobian matrix transforms a small vector difference in control space into the small vector difference in color space. In advanced calculus, the theory of random variables, etc., its determinant gives the ratio of differential volumes in two spaces mapped between by a function. The integral over control space of the Jacobian determinant is somewhat similar to the CRP (color representing power) of Tajima (1983), which gives the number of discernably different colors producible by the machine. The equation defining the Jacobian is:

$$\underline{dC} = \mathbf{J}\,\underline{dK} \tag{5}$$

with **J** the Jacobian matrix

$$\mathbf{J}_{ij} = \frac{\partial C_i}{\partial K_j} \tag{6}$$

where $\underline{C}$ is the CIELUV color vector (L* u* v*)' and $\underline{K}$ is the control vector (r g b)'. (We reserve R, G, and B for the tristimulus primaries to distinguish them from r, g, and b, the control values input to the machine. See the Appendix.) In our case, the units of the Jacobian determinant are cubic JND's per cubic input unit, and it is a measure of how much color volume is used per unit volume in control space. The Jacobian determinant, as well as other quantities based on the Jacobian matrix, are functions of the control vector. That is, it varies as the individual components of the (r g b)' control vector change. We will have use of the norm of the matrix-vector product.

$$|| \mathbf{J} \hat{H} || = \sqrt{\underline{C}'\underline{C}} \tag{7}$$

where $\hat{H}$ is a unit vector and

$$\underline{C} = \mathbf{J} \hat{H} \tag{8}$$

Then $||\mathbf{J}\hat{H}||$ is the amount of color change, measured in JND's, for each unit of control vector difference in the direction $\hat{H}$. Again, note that $||\mathbf{J}\hat{H}||$ is a function of both direction $\hat{H}$ and the control vector $\underline{K}$ at which $\mathbf{J}$ is evaluated.

D. THE JACOBIAN ELLIPSE

We will observe the locus in color space that corresponds to a circular locus in the control space. In that way we show the color difference resulting from a control difference of constant magnitude and varying direction, and we will see that even in a machine mathematically idealized for its on-axis behavior, there is substantial departure from visual uniformity if we do not take into proper account its off-axis behavior. We will take $\hat{H}$ as the unit-length control vector encircling control vector $\underline{K}$, and $\underline{C}$ as the color difference vector resulting from $\hat{H}$. Inasmuch as Equation (8) is a linear form, a plane in K-space maps into a plane in C-space, and generally a circle in K-space becomes an ellipse in C-space. If the machine were uniform, then the circles in K-space would map to circles in C-space. Now the normals to the circles in K-space do not necessarily map to normals of the ellipses in C-space, and also the family of actual normals to the ellipses will not generally all be parallel even if the family of K-space circles have parallel normals. So there is considerable difficulty in displaying the C-space ellipses in a K-space section, let alone actually understanding what is being displayed. In Figures 2a, 3a, and 4a, we have attempted such a display. For circles centered at a grid of K-space locations we have calculated the C-space ellipses. The ellipses' sizes are all scaled by the same factor, and they are brought into the K-space centered on their respective grid locations. The rotational position of the ellipses is specified by projecting the L^* axis onto each ellipse and then placing that direction vertically in the Figure. The horizontal direction thus corresponds to a solely chromatic shift, and the vertical direction will generally comprise some chromatic shift in addition to all the lightness shift. As a data-difference vector swings in a circle around its data center, the color vector moves in its ellipse, the discriminability between the center color and the color on the ellipse being proportional to the distance from the center to the point on the ellipse. The important feature is the considerable eccentricities of the ellipses. The ratio of semi-major axis to semi-minor axis is the ratio by which the discriminability varies. For all the accuracy of a machine set up mathematically per the criteria very often sought in practice, the effects of the machine's off-axis behavior and the experimentally observed color discrimination of the human eye cause enormous variations in the visibilities of data differences themselves having a common size.

E. THE JACOBIAN PEANUT

In an attempt to avoid some of the interpretation difficulties of the Jacobian ellipse display, we have created the graph we call the Jacobian peanut. To make it, a unit data-difference vector is swung in a circle around a control center, just as in making the Jacobian ellipses. The unit data-difference vector is multiplied by the norm of the corresponding color-difference vector. The polar plot around each control center has its angle in the direction of the data-difference vector and its radius proportional to the observed color difference. The shape of the plot bears a resemblance to the seed for which it is named, with the varying eccentricity of the Jacobian ellipse determining how strongly pinched the waist of the peanut is. In the Jacobian peanut, direction has more directly discernible import than in the ellipse;

it is the actual direction of the data difference vector. In the peanut plot, angles are preserved at the expense of color-difference fidelity between pairs of data difference vectors. In the ellipse plot the pair fidelity is maintained at the expense of angular fidelity; you can't have it both ways.

The shape of the peanut plot is made plausible by noting the relative azimuthal angles in the K-space circle and in the Jacobian ellipse. A typical ellipse is shown in Figure 5. As the data-difference vector swings around at constant rate, the corresponding point on the Jacobian ellipse spends a larger amount of time near the semi-major axis of the ellipse than near the semi-minor axis. The points crowded together near the semi-major apex are individually well discriminable from the center color, though they are not so well mutually discriminable. As the data-difference vector in K-space swings through the direction of minimum discriminability, the angle in the Jacobian ellipse races through the semi-minor axis and its lesser norm. The result is a peanut shape for the polar plot.

Another plausibility argument is based on considering the peanut plot character if only one direction in the K-space circle gave any visible color difference. The Jacobian ellipse collapses to a line. The sensitive component of a K-space difference vector circle has cosine dependence, which plots as a circle passing through the origin. Color difference is an absolute magnitude quantity, and abs(cos(•)) makes a figure-8. Indeed the highly eccentric ellipses make peanuts that are nearly figure-8's.

F. DISCUSSION OF THE GRAPHS

In Figure 1 we show that density linearization is a step toward making a color machine uniform; the tick marks occur at more nearly even intervals for density linearization than they do for radiance linearization. This is particularly true away from the origin's vicinity. To make the Figure, a point is slid along a control axis away from the control space origin and marks are placed at UCS intervals of 30 JND as measured from the origin. The tick marks for the density linearizations do not begin at as low values of control as for radiance linearization, particularly for the larger D_{max}. A larger value of D_{max} allows more different colors to be expressed. This is illustrated by the larger values of the maximum color distance at the "fully-on" edge of Figure 1. Smaller D_{max} means that all three primaries remain "on" to a larger degree, so one cannot make the colors near the edges of the Maxwell triangle, as the opposite primary desaturates the color by remaining on. Radiance linearization permits the entirety of the Maxwell triangle to be made.

In Figures 2 through 5 we extend the on-axis results of Figure 1 into the plane section of the control cube having red control of 0.5. (Similar results are obtained for sections of constant green or constant blue control, so they are not shown here.)

Referencing Figure 2 we see that sensitivity to a control is uniformly reduced as the other controls are turned on; the ellipses and peanuts shrink as we move to the right or upward. (A similar effect ensues from changing the red control, not shown here.) In Figure 3b there is little sensitivity to a blue change in the lower right corner (the peanut lies on its side), and as the blue value is increased (move toward the upper right corner) both blue and green differential sensitivities increase. In the upper right corner there is more sensitivity to a change in the blue/green balance (principally a chromatic shift) than there is to the blue+green sum (principally a lightness shift). The effect is more strongly present in Figure 4b with its larger D_{max}.

The major point is that the behavior is a function of both control variables; the visibility of a green control change is affected by the value of the red control.

In Figure 5 we see the root of the peanut behavior for the directional sensitivity plots; as a control-difference vector swings smoothly through a circle the color-difference vectors linger near the semi-major extremes of the Jacobian ellipse. The radials in the Figure are at uniformly spaced azimuths in the control space, yet they bunch near the apices of the ellipse. Those clustered points are individually well distinguishable from the center, but they are not well distinguishable from each other. That feature is apparent in the ellipse plots but is obscured in the peanut plots, so both kinds of plots have been presented.

G. APPENDIX

The color machine has primary tristimulus values in matrix form

$$\mathbf{M} = \begin{pmatrix} X_R & X_G & X_B \\ Y_R & Y_G & Y_B \\ Z_R & Z_G & Z_B \end{pmatrix} = \begin{pmatrix} 58.79 & 17.92 & 18.31 \\ 28.96 & 60.58 & 10.46 \\ 0.0 & 6.83 & 102.02 \end{pmatrix}$$

chosen to give the NTSC chromaticities

$$\begin{pmatrix} x_R & x_G & x_B \\ y_R & y_G & y_B \end{pmatrix} = \begin{pmatrix} 0.67 & 0.21 & 0.14 \\ 0.33 & 0.71 & 0.18 \end{pmatrix}$$

and balance to the D65 illuminant $\underline{T}_o = (X_o \; Y_o \; Z_o)'$ with chromaticity

$$\begin{pmatrix} x_o \\ y_o \end{pmatrix} = \begin{pmatrix} 0.3128 \\ 0.3292 \end{pmatrix}$$

from which it follows that

$$\underline{T}_o = \begin{pmatrix} X_o \\ Y_o \\ Z_o \end{pmatrix} = \begin{pmatrix} 95.018 \\ 100.000 \\ 108.842 \end{pmatrix} .$$

For radiance linearization the control vector

$$\underline{K} = \begin{pmatrix} r \\ g \\ b \end{pmatrix}$$

with $0 \le r \le 1$, $0 \le g \le b$, $0 \le b \le 1$ produces the tristimulus vector

$$\underline{T} = \begin{pmatrix} X \\ Y \\ Z \end{pmatrix} = \mathbf{M} \, \underline{K}.$$

For density linearization, define

$$a_R = 10 ** [-(1 - r) D_{max}]$$

and similarly for a a_G and a_B, with D_{max} thus the largest density (defined as the negative of the $\log_{10}$ of radiance ratio) producible by the machine -- identical D_{max} for all three primaries is assumed. Defining

$$\underline{A} = \begin{pmatrix} a_R \\ a_G \\ a_B \end{pmatrix}$$

then

$$\underline{T} = \mathbf{M}\,\underline{A}$$

We choose the CIELUV coordinate system to express a color; neglecting the expressions for extremely low lightnesses,

$$\underline{C} = \begin{pmatrix} L^* \\ u^* \\ v^* \end{pmatrix}$$

where

$$u' = \frac{4X}{X + 15Y + 3Z}$$

$$v' = \frac{9Y}{X + 15Y + 3Z}$$

and u_o, v_o are the values gotten from $\underline{T}_o$.

Finally,

$$L^* = 116\left(\frac{Y}{Y_o}\right)^{1/3} - 16$$

$$u^* = 13 \quad L^* \left(u' - u_o'\right)$$

$$v^* = 13 \quad L^* \left(v' - v_o'\right)$$

We thus have a(n invertible) relationship between the control vector $\underline{K}$ and the color vector $\underline{C}$. We selected the CIELUV system as being reasonably uniform and having a chromaticity diagram.

The Jacobian matrix has as its (i,j) element the partial derivative

$$\mathbf{J}_{i,j} = \frac{\partial C_i}{\partial K_j}$$

which was approximated by the ratio of finite differences.

A small sphere in K - space becomes an ellipsoid in C - space according to

$$\underline{dC} = \mathbf{J}\ \underline{dK}$$

and the ellipsoid is given by the quadratic form

$$\frac{\underline{dC}^T\ \underline{dC}}{\underline{dK}^T\ \underline{dK}} = \frac{\underline{dK}^T\ \mathbf{J}^T\ \mathbf{J}\ \underline{dK}}{\underline{dK}^T\ \underline{dK}} \quad .$$

For a full volume examination (contrasted with the plane sections done in this paper) one observes the eigenvectors of the full-rank (for any practical color machine) symetric matrix $\mathbf{R} = \mathbf{J}^T\mathbf{J}$. The eigenvectors of $\mathbf{R}$ point in the directions of the axes of the ellipsoid, but the eigenvalues of **R** are not directly usable. A symmetric decomposition of **R** can produce usable values on the diagonal, but in practice we obtain the lengths of the ellipsoid diagonals as follows.

Let $\mathbf{E} = (\underline{e}_1\ \underline{e}_2\ \underline{e}_3)$ be the matrix of orthonormal eigenvectors of **R** corresponding to the eigenvalues of **R**, $\lambda_1, \geq \lambda_2 \geq \lambda_3$. Then

$$P_i = \| \mathbf{J}\underline{e}_i \|$$

is the length of the i^{th} semi-axis of the ellipsoid, and we can calculate the maximum eccentricity

$$E_{max} = \sqrt{1 - \frac{P_3}{P_1}}$$

of any ellipse that is a plane section of the ellipsoid. E_{max} is a function of $\underline{K}$ and is a measure of the color machine's non-uniformity without regard to a pre-determined orientation of a cutting plane.

The ellipses shown here result from oriented small circles in the control space, however, rather than from spheres and ellipsoids.

Let $\hat{n}$ be a unit vector normal to the circle [for a circle in a plane of constant red control value, $\hat{n} = (1\ 0\ 0)'$, etc.], and let $\hat{t}$ and $\hat{u}$ complete an orthonormal basis in K-space. Let $\underline{K}_o$ be the center of the circle. The following algorithm creates the ellipses in C-space and carries them to K-space with (arbitrarily) the projection of L^* into the C - space ellipse aligned with $\hat{t}$.

$$\mathbf{A} = (\underline{v} \quad \underline{z} \quad \underline{w}) = \mathbf{J}\,(\hat{n} \quad \hat{t} \quad \hat{u})$$

$$\beta = \mathbf{A}^{-1}\begin{pmatrix}1\\0\\0\end{pmatrix}$$

$$\underline{\mu} = \begin{pmatrix}0\\ \beta_2\\ \beta_3\end{pmatrix}$$

$$\hat{d} = \frac{\underline{\mu}}{\|\underline{\mu}\|}$$

$$a = \left\{ \underline{z}^T\underline{z} - 2\,\frac{(\hat{d}^T\underline{z})(\underline{z}^T\underline{w})}{(\hat{d}^T\underline{w})} + \left(\frac{\hat{d}^T\underline{z}}{\hat{d}^T\underline{w}}\right)^2 \underline{w}^T\underline{w} \right\}^{1/2}$$

$$b = -a\,\frac{\hat{d}^T\underline{z}}{\hat{d}^T\underline{w}}$$

$$\hat{\varphi} = a\,\underline{z} + b\,\underline{w}$$

$$\hat{\delta} = \hat{d} \times \hat{\varphi}$$

$$\mathbb{B} = (\hat{d} \quad \hat{\varphi} \quad \hat{\delta})$$

$$\underline{f} = \mathbb{B}^{-1}(\underline{z}\cos\theta + \underline{w}\sin\theta), \qquad \theta \in [0, 2\pi]$$

Plot

$$\underline{K} = \underline{K}_o + F \cdot (\hat{t} f_1 + \hat{u} f_2)$$

for a suitable scale factor F.

The peanuts are rather simpler. One merely plots

$$\underline{K} = \underline{K}_o + F \cdot \| \mathbb{J} \underline{\rho} \| \underline{\rho}$$

where

$$\underline{\rho} = \hat{t} \cos\theta + \hat{u} \sin\theta \, , \quad \theta \in [0, 2\pi]$$

again, for a suitable scale factor F.

FIGURE CAPTIONS

Figure 1. Tick marks at intervals of 30 JND (just-noticeable difference; see text) plotted for the red, greeen, and blue axes. Maximum color difference as measured from the origin is given. The color machine is linearized in radiance or in density. Density linearization causes more even placement of the ticks. The number of distinguishable colors on an axis is proportional to its number of ticks, so a lower D_{max} reduces the number of different colors.

Figure 2. Jacobian ellipses and peanuts for radiance linearization; the plane is red = 0.5. In comparison with density linearization (see the next two Figures) the largest discriminability occurs at low values of color control, eccentricity of ellipses is small, and there is low contrast over much of the area.

Figure 3. Jacobian ellipses and peanuts for density linearization, taken in the red = 0.5 plane and with D_{max} = 1.0. In comparison with the larger D_{max} of the next figure, the ellipses have less eccentricity and less variation in their size. Less total color volume is available, however, so the cost is lower maximum contrast.

Figure 4. Jacobian ellipses and peanuts for density linear-

ization, taken in the red = 0.5 plane with D_{max} = 2.0. The large color range available with the large D_{max} is at the cost of considerable eccentricity and variation in size of the ellipses. Note in this and the previous two figures that sensitivity to changes in a control value is strongly a function of the other control value.

Figure 5. An enlargement of a Jacobian ellipse showing radials that are at equal azimuth intervals in control space. This ellipse is the image in color space of a small circle in control space. Visual discriminability is largest along those control space directions that transform near the major axes of the ellipse. The bunching of the radials is responsible for the shape of the Jacobian peanuts.

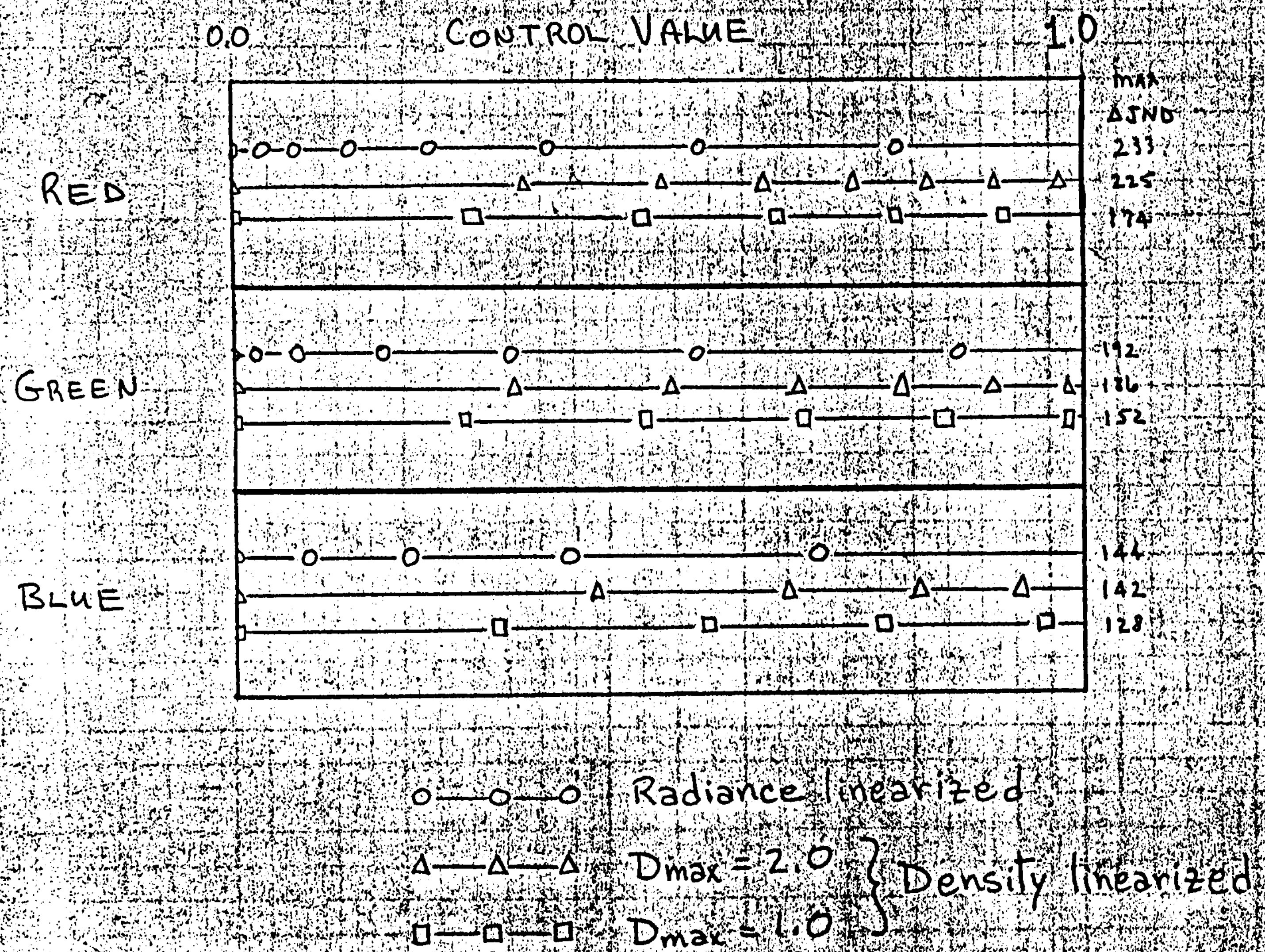
0.0
CONTROL VALUE
1.0
MAX
ΔSND
233
225
174
192
186
152
144
142
128
RED
GREEN
BLUE
Radiance linearized
Dmax = 2.0
Dmax = 1.0
Density linearized

FIGURE 1

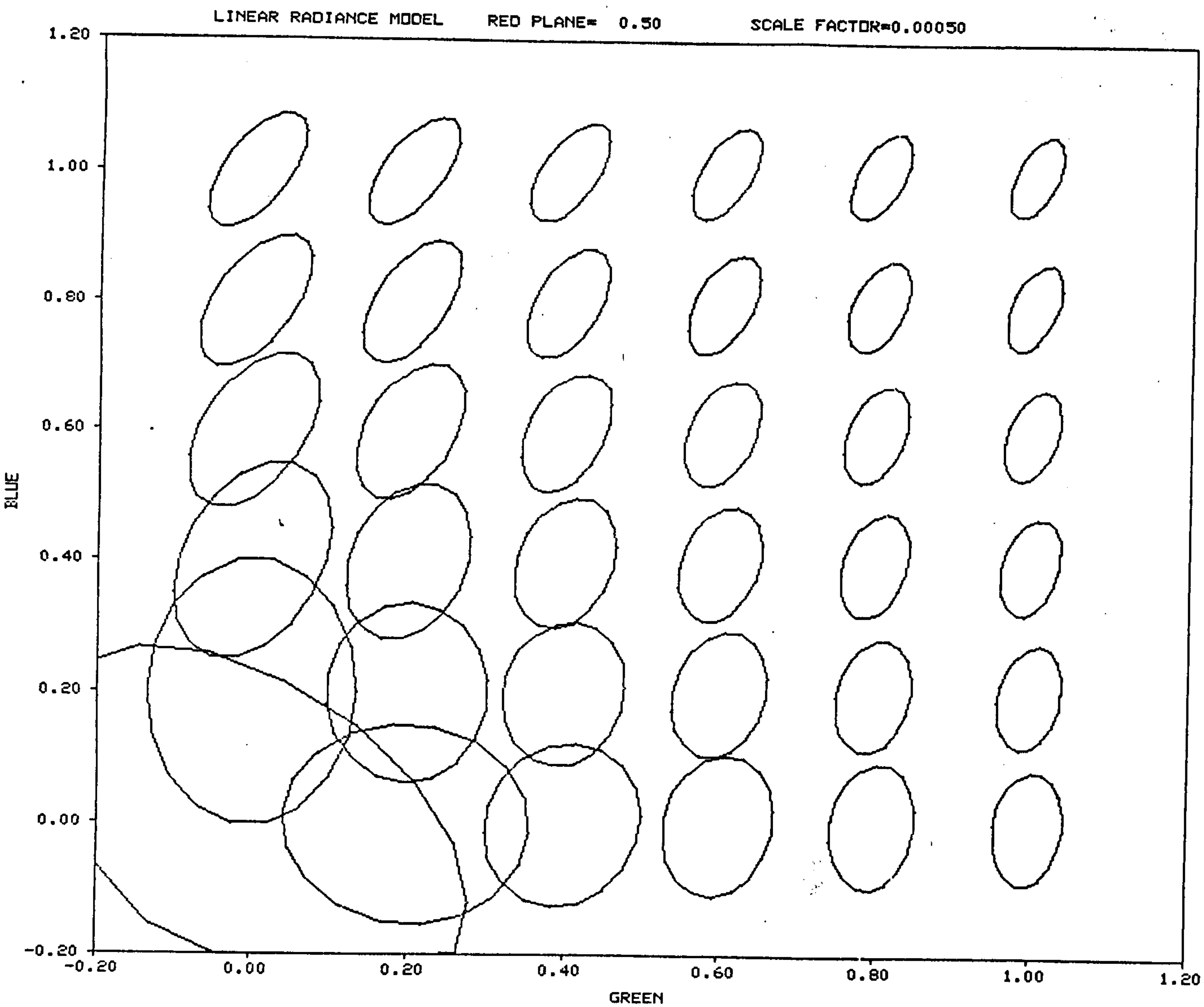
LINEAR RADIANCE MODEL
RED PLANE= 0.50
SCALE FACTOR=0.00050
BLUE
GREEN
1.20
1.00
0.80
0.60
0.40
0.20
0.00
-0.20

FIGURE 2a

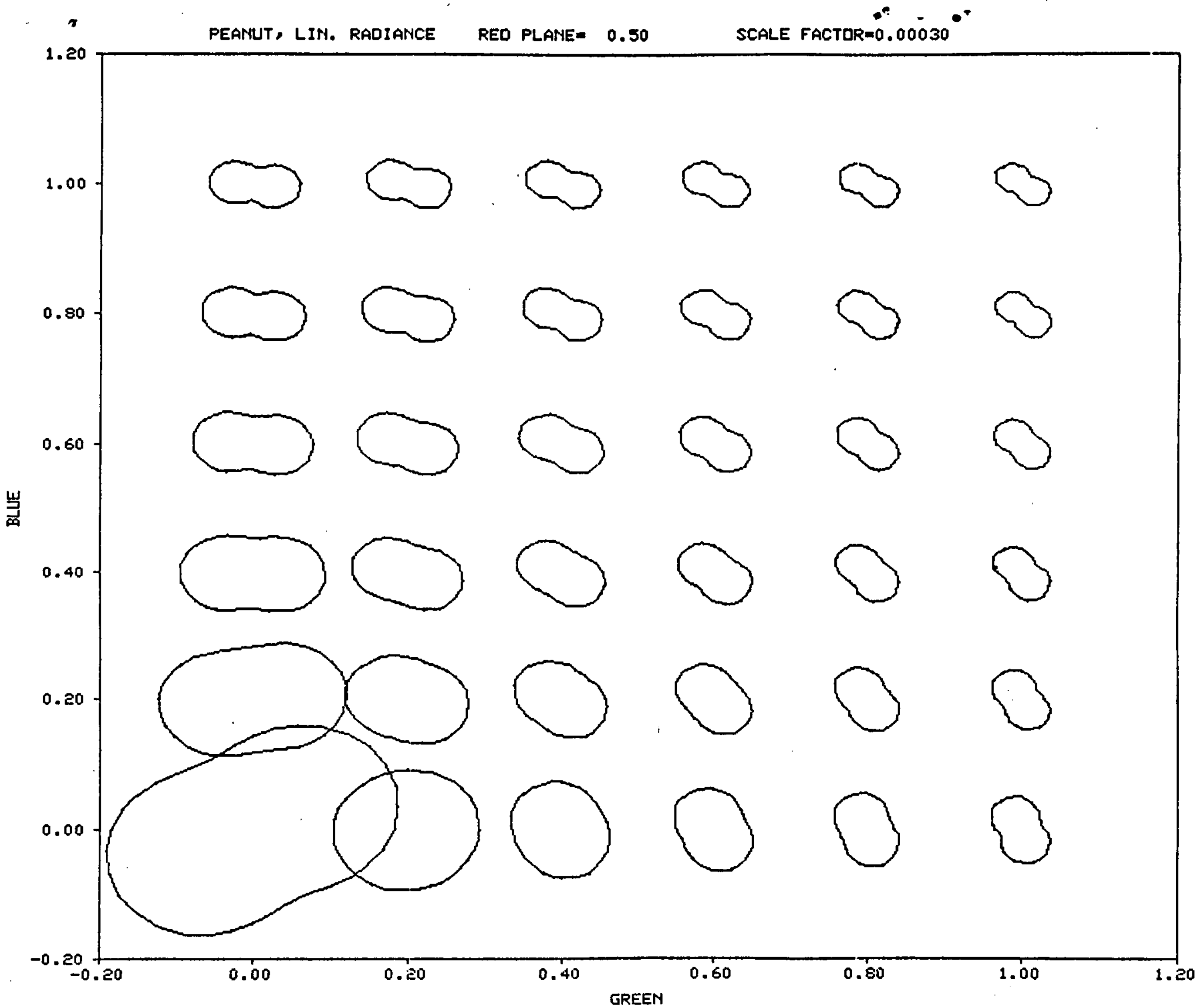

PEANUT, LIN. RADIANCE RED PLANE= 0.50 SCALE FACTOR=0.00030
BLUE
GREEN
1.20
1.00
0.80
0.60
0.40
0.20
0.00
-0.20
-0.20
0.00
0.20
0.40
0.60
0.80
1.00
1.20

FIGURE 2b

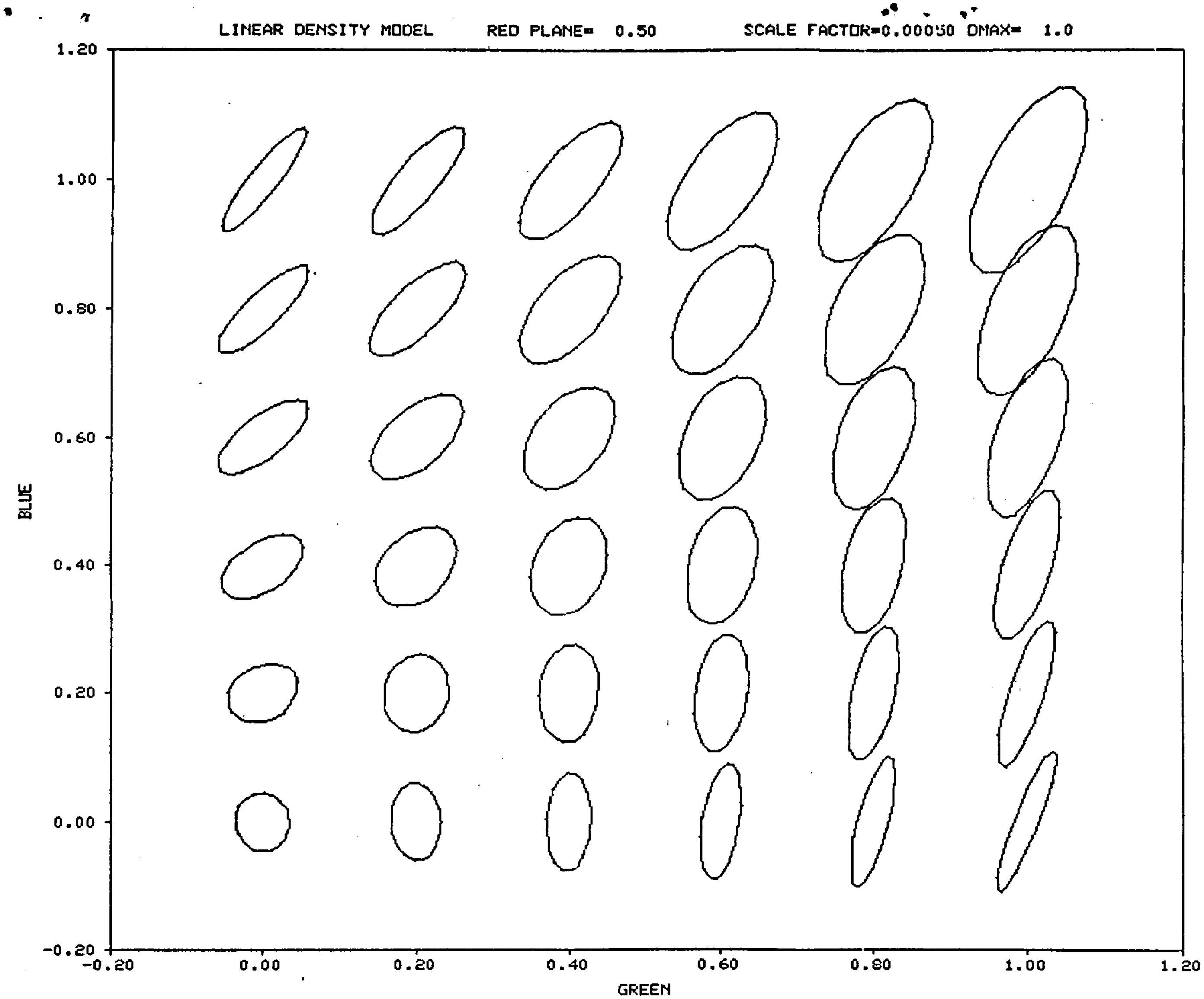
LINEAR DENSITY MODEL
RED PLANE= 0.50
SCALE FACTOR=0.00050 DMAX= 1.0
1.20
1.00
0.80
0.60
0.40
0.20
0.00
-0.20
BLUE
-0.20
0.00
0.20
0.40
0.60
0.80
1.00
1.20
GREEN

FIGURE 3a

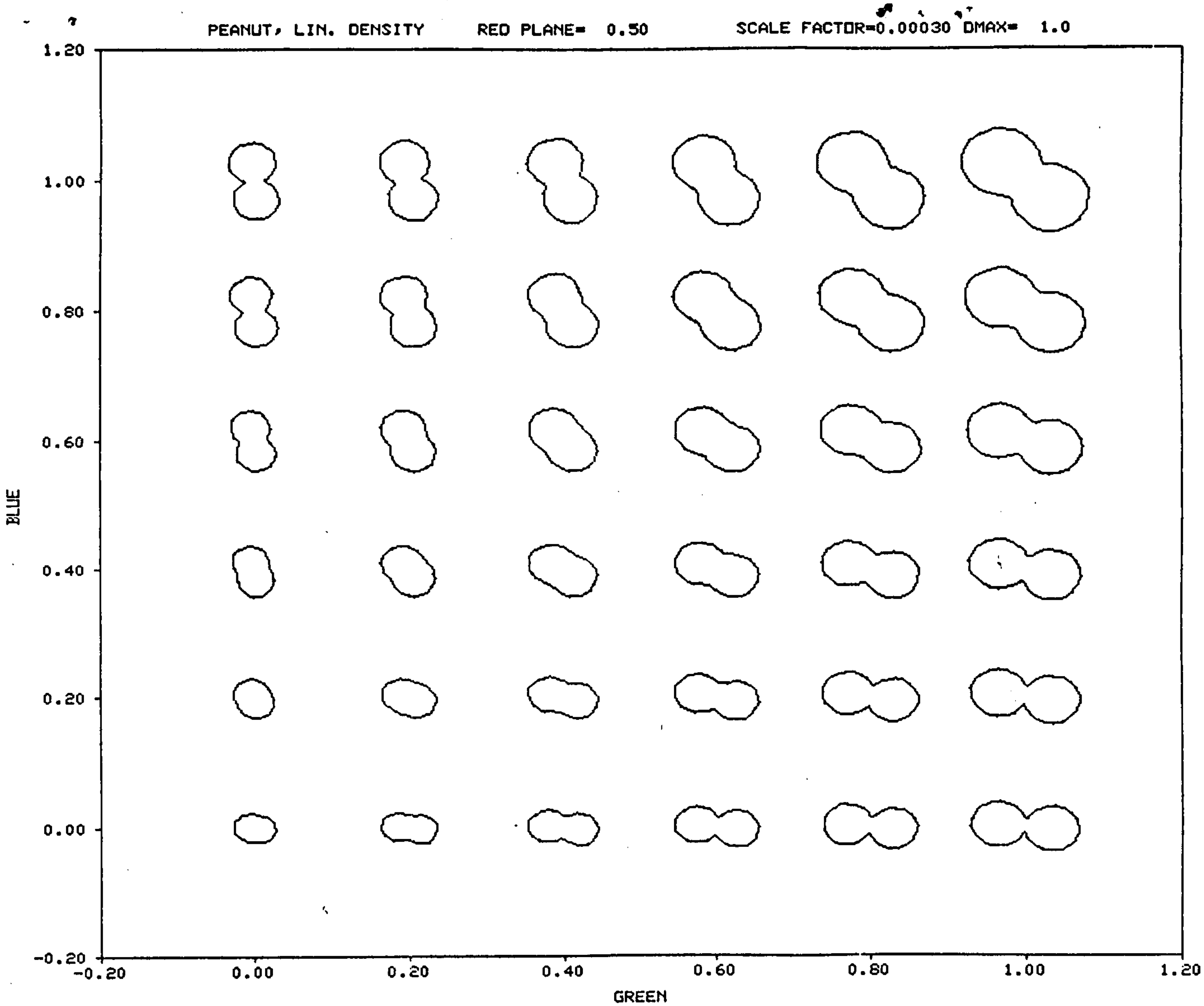
PEANUT, LIN. DENSITY
RED PLANE= 0.50
SCALE FACTOR=0.00030 DMAX= 1.0
BLUE
1.20
1.00
0.80
0.60
0.40
0.20
0.00
-0.20
-0.20
0.00
0.20
0.40
0.60
0.80
1.00
1.20
GREEN

FIGURE 3b

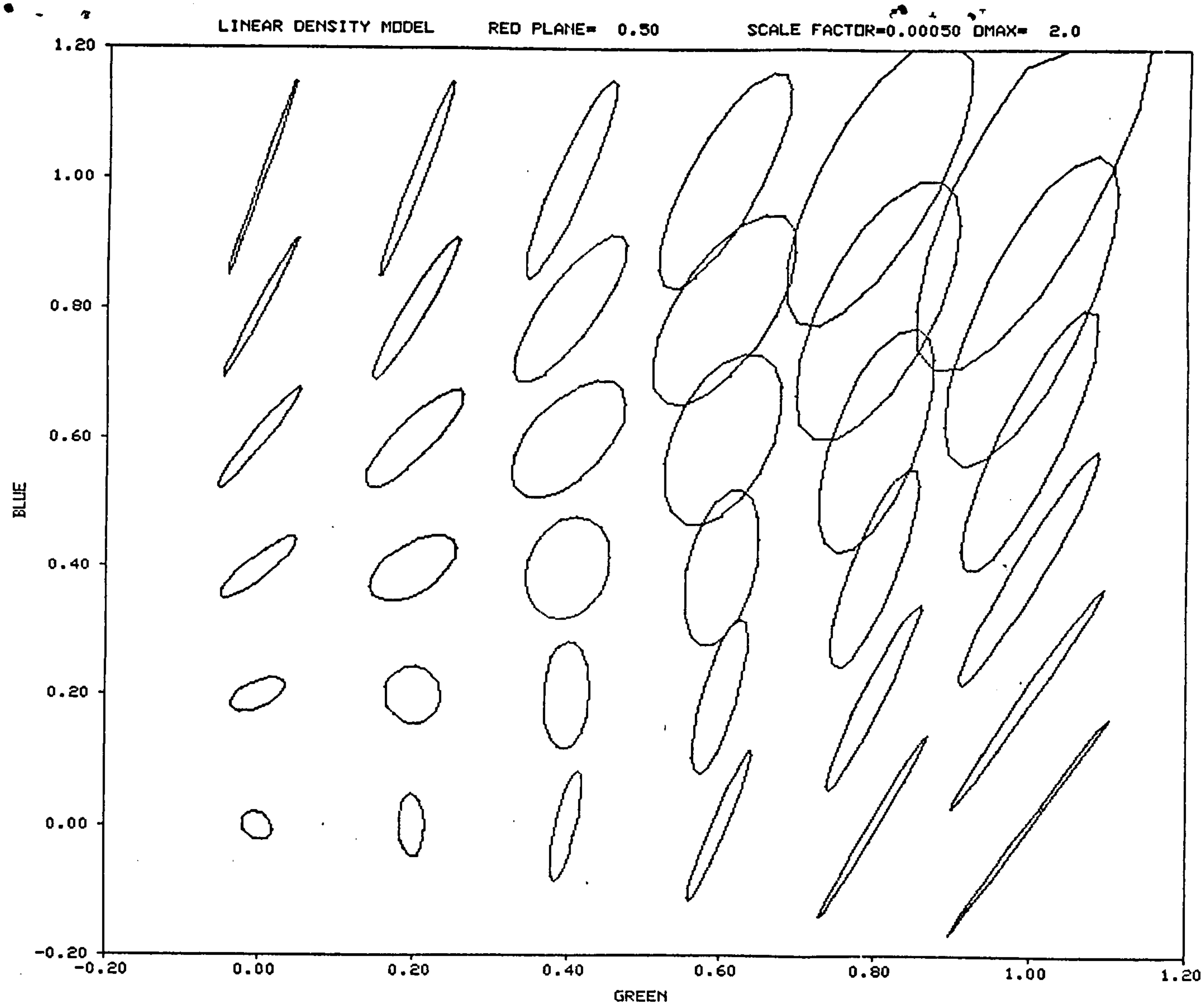
LINEAR DENSITY MODEL
RED PLANE= 0.50
SCALE FACTOR=0.00050 DMAX= 2.0
BLUE
GREEN
-0.20
0.00
0.20
0.40
0.60
0.80
1.00
1.20

FIGURE 4a

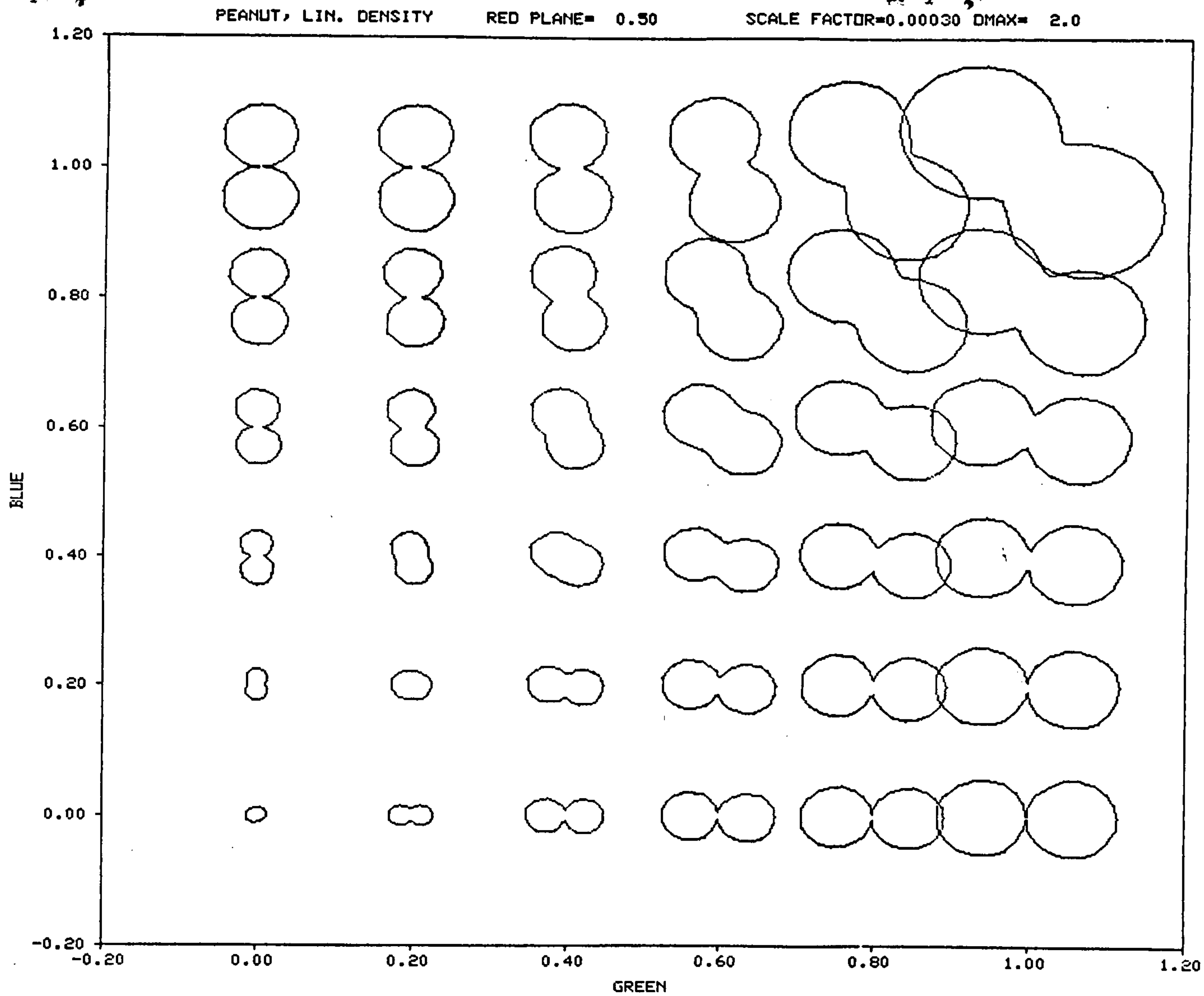
PEANUT, LIN. DENSITY
RED PLANE= 0.50
SCALE FACTOR=0.00030 DMAX= 2.0
BLUE
1.20
1.00
0.80
0.60
0.40
0.20
0.00
-0.20
-0.20
0.00
0.20
0.40
0.60
0.80
1.00
1.20
GREEN

FIGURE 4b

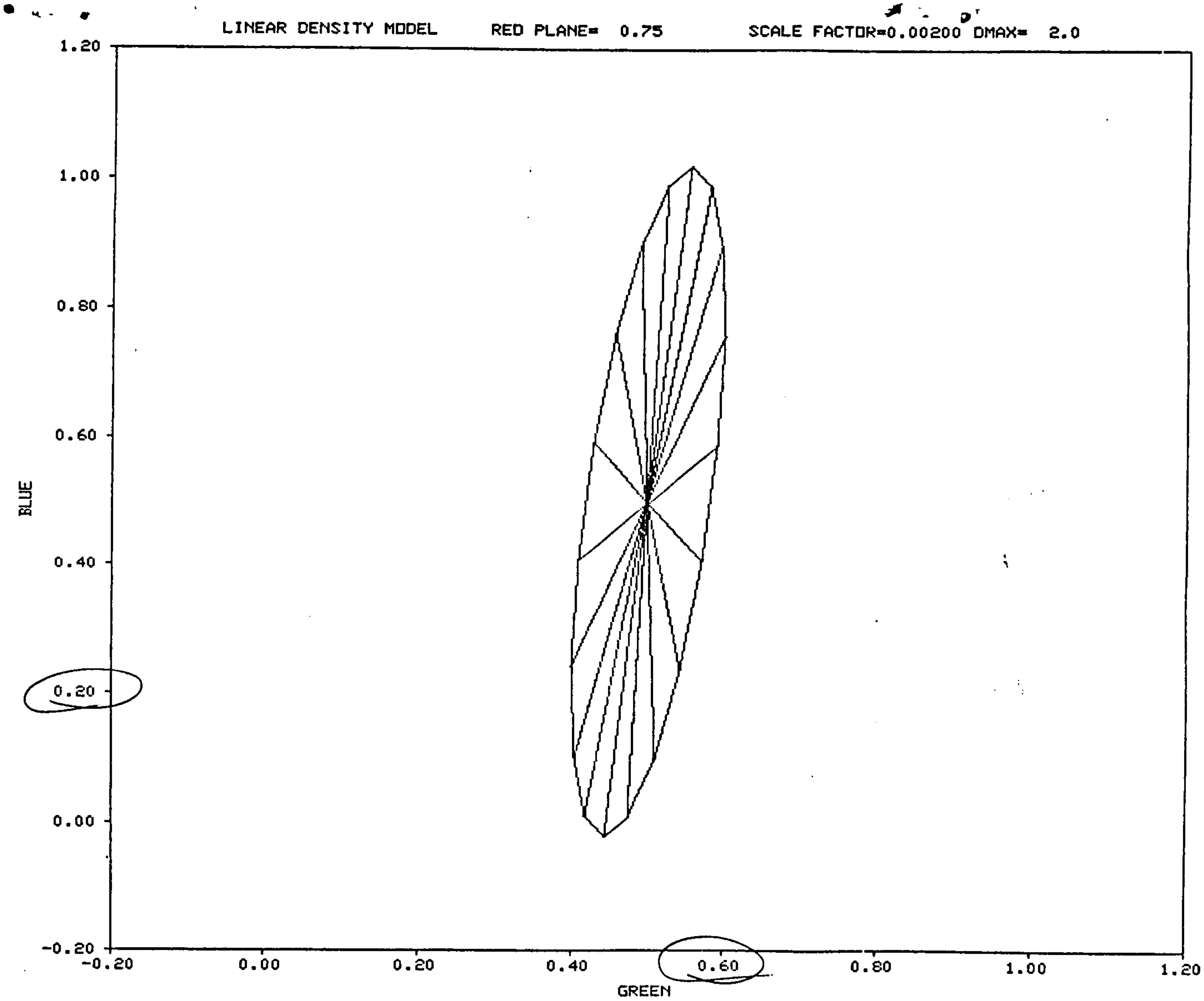
LINEAR DENSITY MODEL
RED PLANE= 0.75
SCALE FACTOR=0.00200 DMAX= 2.0
BLUE
1.20
1.00
0.80
0.60
0.40
0.20
0.00
-0.20
GREEN
-0.20
0.00
0.20
0.40
0.60
0.80
1.00
1.20

FIGURE 5

REFERENCES

Catmull, Edwin, 1979. A tutorial on compensation tables, Computer Graphics 13, 1-7.

Madura, Daryl P., James M. Soha, William B. Green, David B. Wherry, and Stanley D. Lewis, 1978. Color enhancements of Landsat imagery, JPL Publication 78-102, December 15, 1978.

Pratt, W. K., 1978. Digital Image Processing, Wiley, New York.

Soha, James M., Alan R. Gillespie, Michael J. Adams, and Daryl P. Madura, 1976. Computer techniques for geological applications, Proceedings of the Caltech/JPL Conference on Image Processing, Technology Sources, and Software for Commercial and Scientific Applications, November 3-5, 1976. JPL SP 43-30.

Tajima, Johji, 1983. Uniform color scale applications to computer graphics, Computer Vision, Graphics, and Image Processing 21, 305-325.

Wyszecki, Gunter, and W. S. Stiles, 1982. Color Science, Wiley, New York.